LETTERS
PUBLISHED ONLINE: 8 AUGUST 2016 | DOI: 10.1038/NNANO.2016.132
nature nanotechnology

Ultrafast growth of single-crystal graphene assisted by a continuous oxygen supply

Xiaozhi Xu[1,2], Zhihong Zhang[1,2], Lu Qiu[3], Jianing Zhuang[3], Liang Zhang[1], Huan Wang[4], Chongnan Liao[5], Huading Song[1], Ruixi Qiao[1], Peng Gao[1,6], Zonghai Hu[1], Lei Liao[5], Zhimin Liao[1,6], Dapeng Yu[1,2,6,7], Enge Wang[6,8], Feng Ding[3]*, Hailin Peng[2,4,9]* and Kaihui Liu[1,2,4,6]*

Graphene has a range of unique physical properties[1,2] and could be of use in the development of a variety of electronic, photonic and photovoltaic devices[3–5]. For most applications, large-area high-quality graphene films are required and chemical vapour deposition (CVD) synthesis of graphene on copper surfaces has been of particular interest due to its simplicity and cost effectiveness[6–15]. However, the rates of growth for graphene by CVD on copper are less than 0.4 μm s^{-1}, and therefore the synthesis of large, single-crystal graphene domains takes at least a few hours. Here, we show that single-crystal graphene can be grown on copper foils with a growth rate of 60 μm s^{-1}. Our high growth rate is achieved by placing the copper foil above an oxide substrate with a gap of ~15 μm between them. The oxide substrate provides a continuous supply of oxygen to the surface of the copper catalyst during the CVD growth, which significantly lowers the energy barrier to the decomposition of the carbon feedstock and increases the growth rate. With this approach, we are able to grow single-crystal graphene domains with a lateral size of 0.3 mm in just 5 s.

Previous work on growing large-area, high-quality, single-crystal graphene on copper foils has typically focused on suppressing nucleation, and the most successful approach has led to the synthesis of centimetre-sized single crystals of graphene in a day[9]. As the suppression of nucleation is mostly achieved by lowering the feedstock concentration, a common feature of these growth methods is a very low growth rate (0.03–0.36 μm s^{-1}) and therefore a long growth time (hours to days)[7–12]. Crystal nucleation is known to be a quantum probability event, and thus the number of nuclei that form during the whole growth process should be proportional to the total duration of graphene growth. Ultrafast growth would therefore be ideal for the synthesis of graphene films with very large single-crystalline domains, but there so far only been a limited amount of work on improving the growth rate of graphene[16,17].

The ultrafast CVD growth of one-dimensional carbon nanotubes is already possible, and half-metre-long high-quality carbon nanotubes have been synthesized with growth rates of up to 80 μm s^{-1} (ref. 18), which is very close to the theoretical limit[19]. As graphene is a two-dimensional form of such graphitic materials, one would expect a similar growth rate for graphene by the CVD method[20]. However, the best graphene growth rates reported so far are 0.4 μm s^{-1} on Cu foils[6–14], 2.0 μm s^{-1} on SiPt foils[16] and 4.2 μm s^{-1} on CuNi alloys[17]. These rates are notably slower than those of carbon nanotubes and there should therefore be room to enhance the graphene growth rate by CVD, particularly on Cu surfaces.

In previous studies of CVD growth of graphene and carbon nanotubes, the introduction of oxygen to the growth environment plays a crucial, but often mysterious, role[8–10,21,22]. In graphene growth the introduction of oxygen to the Cu foil by pre-annealing can greatly decrease the graphene nucleation density and accelerate the growth rate from 0.03 to 0.28 μm s^{-1} (refs 8–10). However, the accelerated graphene growth rate is still ~100 times slower than that achieved in carbon nanotube growth, probably due to the insufficient and/or discontinuous supply of oxygen to the surface of the Cu catalyst. It is a significant challenge to directly deposit oxygen onto the catalyst surface because the hydrogen in the carrier gas, which is required for CVD growth, can easily react with and eliminate the oxygen before it reaches the catalyst surface.

In our approach, we employed an adjacent oxide substrate to continuously supply oxygen to the surface of the Cu during CVD graphene growth (Fig. 1a,b). The Cu foil was placed above a flat oxide substrate at a distance of ~15 μm (Supplementary Fig. 1a). Previous research has shown that the oxide would slowly release oxygen at high temperature (>800 °C)[23]. To prove this fact, in our experiment we carried out Auger electron spectroscopy (AES) element measurements on the SiO_2/Si substrate (with SiO_2 thickness of ~5 nm) and demonstrated that oxygen escapes from SiO_2 after annealing in either an ultrahigh vacuum system or our CVD system under the growth conditions (Fig. 1c). Despite the small amount of oxygen released, our fluidic model shows that the oxygen concentration in the very narrow gap between the Cu foil and the oxide substrate can be high due to the trapping effect (Supplementary Fig. 1b), and therefore the attachment of oxygen to the surface of the Cu catalyst can be greatly enhanced. In addition to the adjacent supporting oxide substrate, we also use atmospheric pressure, a high CH_4 feeding flow of 5 sccm (standard cubic centimetres per minute) and a high CH_4/H_2 ratio (~1) to further ensure a sufficient supply of carbon for fast graphene growth (see Methods for growth details).

With our design, large circular graphene domains with an averaged lateral size of ~0.3 mm are grown on the back surface of the Cu foil that faces the fused silica within one minute (Fig. 1d). In contrast, most of the observed graphene domains on the front surface of the Cu foil (which is exposed to the open air) are about 20 times smaller, only ~15 μm (Fig. 1e); these smaller domains are also star-shaped. For a control experiment, we use graphite as the

[1]State Key Laboratory for Mesoscopic Physics, School of Physics, Peking University, Beijing 100871, China. [2]Academy for Advanced Interdisciplinary Studies, Peking University, Beijing 100871, China. [3]Institute of Textiles and Clothing, Hong Kong Polytechnic University, Hong Kong, China. [4]Centre for Nanochemistry, College of Chemistry and Molecular Engineering, Peking University, Beijing 100871, China. [5]Department of Physics, Wuhan University, Wuhan 430072, China. [6]Collaborative Innovation Centre of Quantum Matter, Beijing 100871, China. [7]Department of Physics, South University of Science and Technology of China, Shenzhen 518055, China. [8]International Center for Quantum Materials, Peking University, Beijing 100871, China. [9]Beijing Science and Engineering Centre for Nanocarbons, Beijing 100871, China. *e-mail: fengding@polyu.edu.hk; hlpeng@pku.edu.cn; khliu@pku.edu.cn

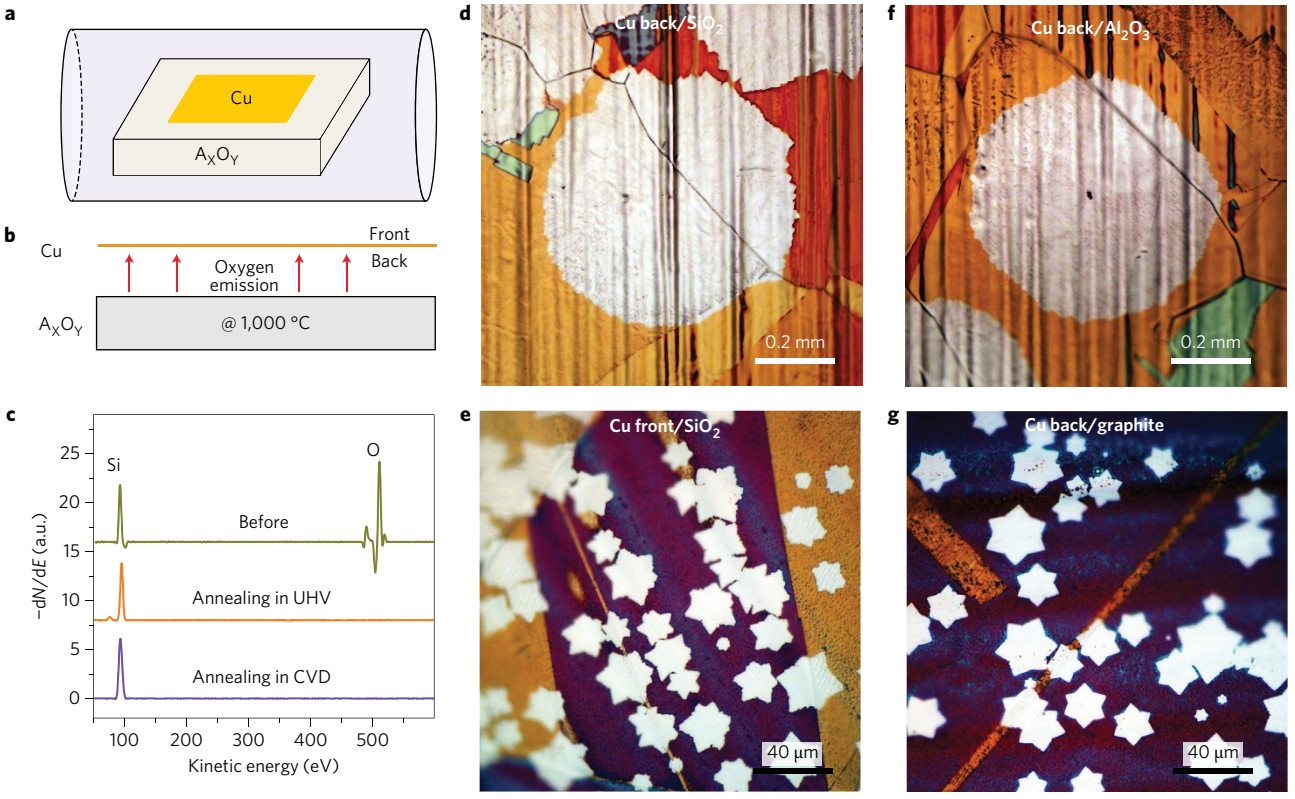

Figure 1 | Growth of graphene on Cu foils assisted by a continuous oxygen supply. a, Schematic of experimental design. **b**, Side view of **a**. A_XO_Y denotes the oxide. **c**, AES of the SiO_2/Si substrate (SiO_2 thickness ~5 nm) before and after annealing at ~1,000 °C in an ultrahigh vacuum (UHV) and CVD systems. The disappearance of the oxygen peak after annealing proves the emission of oxygen from the oxide at high temperature. **d**,**e**, Optical images of graphene domains on the back (**d**) and front (**e**) surfaces of the Cu foils using fused silica as the supporting substrate. **f**,**g**, Optical images of graphene domains on the back surfaces of Cu foils using Al_2O_3 (**f**) or graphite (**g**) as the supporting substrate. The non-oxide graphite does not emit oxygen during the growth process and the graphene domain is as small as 15 μm. The Cu foil is post-treated in air at 200 °C for 5 min after growth for optical visualization of the graphene domains.

supporting substrate and find that the graphene domains on both sides of the foil grow in small star-like shapes (Fig. 1g). We also tried other different oxides of sapphire (Fig. 1f), 300 nm SiO_2/Si (Supplementary Fig. 2a) and quartz (Supplementary Fig. 2b) and found that all of the oxides show a nearly identical effect on graphene growth. In contrast with experiments where oxide is used as a supporting material, the growth behaviours of graphene on both side of the Cu foils are very similar if non-oxide supporting materials, such as Ta (Supplementary Fig. 2c) or SiC (Supplementary Fig. 2d), are used. Summarizing the above results, we can conclude that oxygen released from the oxide close to the back surface of the Cu foil plays a key role in realizing the fast growth of large circular graphene domains.

To verify that the large graphene domains are single crystals, we conducted transmission electron microscopy (TEM) and selected-area electron diffraction (SAED) measurements on individual domains. Figure 2a is the scanning electron microscopy (SEM) image of a typical transferred graphene domain on a TEM grid (see Methods for the transfer procedures). Figure 2b–d shows three representative diffraction patterns that correspond to the areas labelled T_1, T_2 and T_3 in Fig. 2a. The nearly identical crystallographic orientations of the diffraction patterns reveal the single-crystal nature of the graphene domain. This single crystallinity can also be proven by the low-energy electron diffraction (LEED) technique (Fig. 2e–h), whose spot size is around 0.1 mm, providing larger-scale structural information than SAED (spot size: ~0.1 μm).

Atomic-resolution scanning tunnelling microscopy (STM) was employed to verify the quality of the graphene. Figure 2i–k shows three representative STM images in different areas of a domain on the Cu foil. All of the identified carbon atoms are in a honeycomb lattice and no defect is found, which reveals the high quality of the as-grown graphene. Further Raman spectroscopy (Fig. 2l) and mapping (Supplementary Fig. 3) reveal that our graphene has no D peak at the detected level, which is another indication of the high quality.

The measured Hall mobility of graphene domains transferred onto SiO_2/Si substrates is around 4,500–6,500 $cm^2\ V^{-1}\ s^{-1}$ at 1.4 K (Supplementary Fig. 4). This value is close to most of reported values for CVD graphene and also comparable to our exfoliated graphene with the same transfer process applied. Here we note that the obtained mobility values of CVD graphene are highly related to the transfer processes, which may easily bring random impurities and/or strain distribution to the sample and therefore decrease the measured mobility significantly[24–26]. In most cases, the measured mobility does not directly reflect the quality of the as-grown graphene. (If the transfer process can be closely controlled, the mobility of CVD graphene can reach 350,000 $cm^2\ V^{-1}\ s^{-1}$, rivalling that of exfoliated graphene[25]). In this context, it is more reasonable to use STM and Raman data to evaluate the quality of the as-grown CVD graphene without any transfer process.

To obtain the growth rate quantitatively, we took optical images *ex situ* at a certain growth time (Fig. 3a–c). A facile post-oxidation method is used to make the graphene optically visible[27]. The time $t = 0$ is defined as the moment when the graphene domain is large enough to be visualized clearly by optical microscopy (~2 μm). At time t, we stop the furnace heating and CH_4 feeding and immediately allow a large flow of Ar to flush in. We find that the graphene growth rate is ultrafast—in just 5 s, the domain size reaches

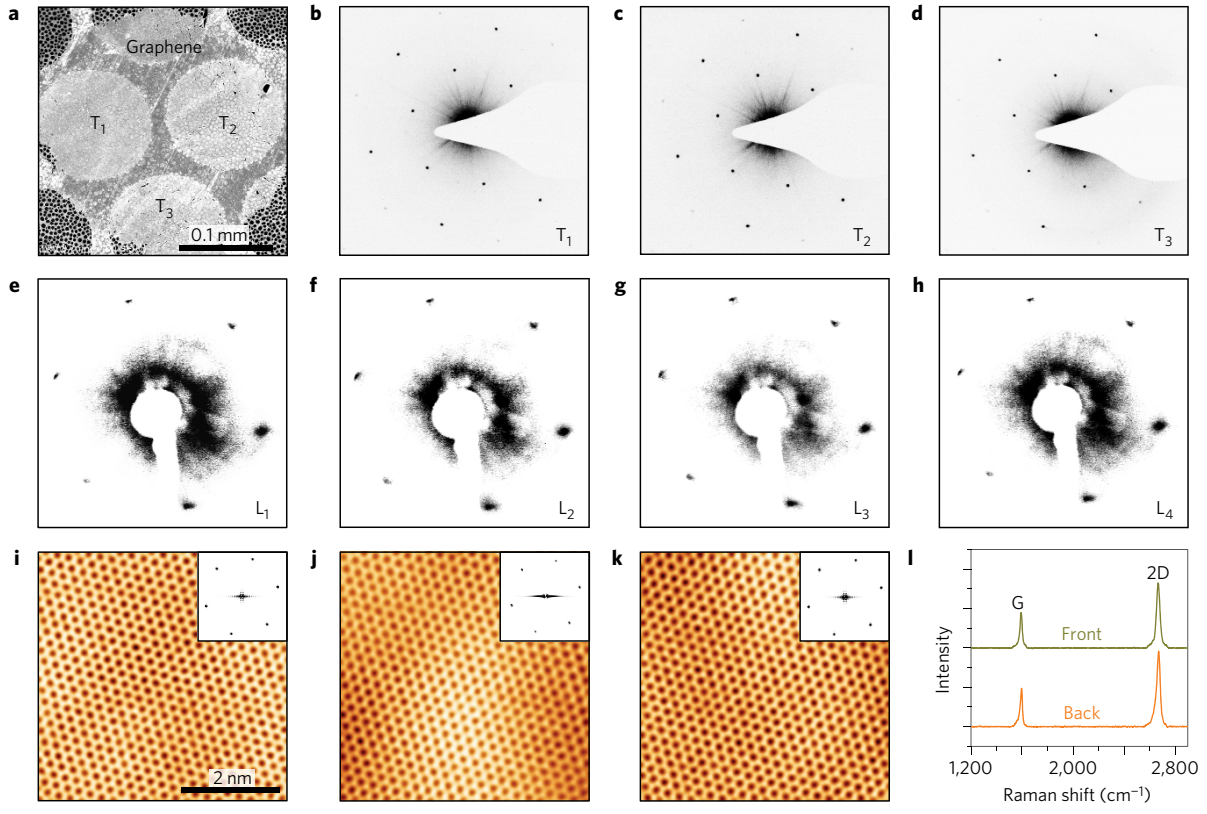

Figure 2 | Single-crystal confirmation and quality characterization of the as-grown graphene domains. a, SEM image of a representative graphene domain transferred onto a TEM grid. **b**–**d**, SAED patterns from the areas labelled T_1 (**b**), T_2 (**c**) and T_3 (**d**) in **a**. **e**–**h**, LEED patterns of a typical graphene domain from area L_1 (**e**), L_2 (**f**), L_3 (**g**) and L_4 (**h**). The nearly identical crystallographic orientations in both the SAED and LEED patterns reveal the single-crystal structure in the individual graphene domains. **i**–**k**, Three representative STM images in different areas of a typical graphene domain on a Cu foil. Insets: fast Fourier transformation patterns. **l**, Raman spectra of graphene on both sides of the Cu foils. The absence of atomic defects in the STM images and non-detectable D peak in the Raman spectra reveal the high quality of the as-grown graphene.

~300 μm (Fig. 3a–c) and the average growth rate is ~60 μm s^{-1} (Fig. 3d), which is close to the theoretical limit[19]. Such a growth rate is several orders of magnitude faster than previous reported rates (see Supplementary Table 1 for comparison to previous values on Cu foils). As also shown in Fig. 3d, the growth rate is constant at different growth times, which is in sharp contrast to the self-limited growth of graphene on a Cu surface, where the growth rate keeps decreasing with increasing graphene coverage[28]. Nonlinear self-limited growth was previously attributed to the low carbon flux during graphene CVD growth and is in agreement with fractal or star-like graphene domain shapes[29]. Here both the constant growth rate and the ultrafast growth clearly indicate that the carbon flux in our experiment is greatly enhanced.

We further checked the evolution of the graphene coverage with time and found a quadratic dependent behaviour (Fig. 3e) where

$$A \sim t^2 \quad (1)$$

as the coverage is proportional to the summation of all of the graphene domains on the surface and the area of a domain is proportional to the square of its growth time. We thus have the total coverage

$$A = \Sigma A_i \sim \Sigma(t - t_i)^2 \quad (2)$$

where t_i is the time at which a new domain nucleates on the Cu surface. Comparing equation (1) with equation (2), we conclude that $t_i = 0$ or that the nucleation during the growth process is negligible, which is one obvious merit of ultrafast growth.

The ultrafast graphene growth is associated with the evolution of the domain shape. We first performed a series of phase-field theory (PFT) simulations to achieve deep insight into the mechanism that governs the shape evolution of the CVD graphene domains (see Supplementary Method 1 for the simulation details). Figure 4a–c and Fig. 4d–f respectively show the simulated graphene domains and corresponding distributions of the carbon precursor concentration on the catalyst surface under various carbon fluxes (F). It can be seen that very low F value (Fig. 4a, $F = 0.001$) leads to a fractal-shaped graphene domain and, with increasing F the domain gradually becomes star-shaped (Fig. 4b, $F = 0.1$) and then a rounded hexagonal shape (Fig. 4c, $F = 4$). As shown in Fig. 4i, the time required to grow a domain with 1/4 coverage on the surface decreases by two orders of magnitude when the carbon flux increases from 0.001 to 4. This simulation result clearly indicates that, without altering the other parameters of growth, the carbon flux controls both the shape of the graphene domains and the growth rate and therefore is very possibly the key mechanism that governs the ultrafast growth. As shown in Fig. 4d–h, there is a large depletion zone at the grown edge of the graphene (where the carbon concentration is significantly lower than that in the area far from it) when the carbon flux is very low ($F = 0.001$). In the case of graphene growth with a very large carbon flux ($F = 4$), the depletion zone becomes negligible and every part of the domain edge is surrounded by equally supersaturated carbon species. With the disappearance of the depletion zone, the mode of graphene growth undergoes a change from diffusion-limited growth to attachment-limited growth, as evidenced by the evolution of

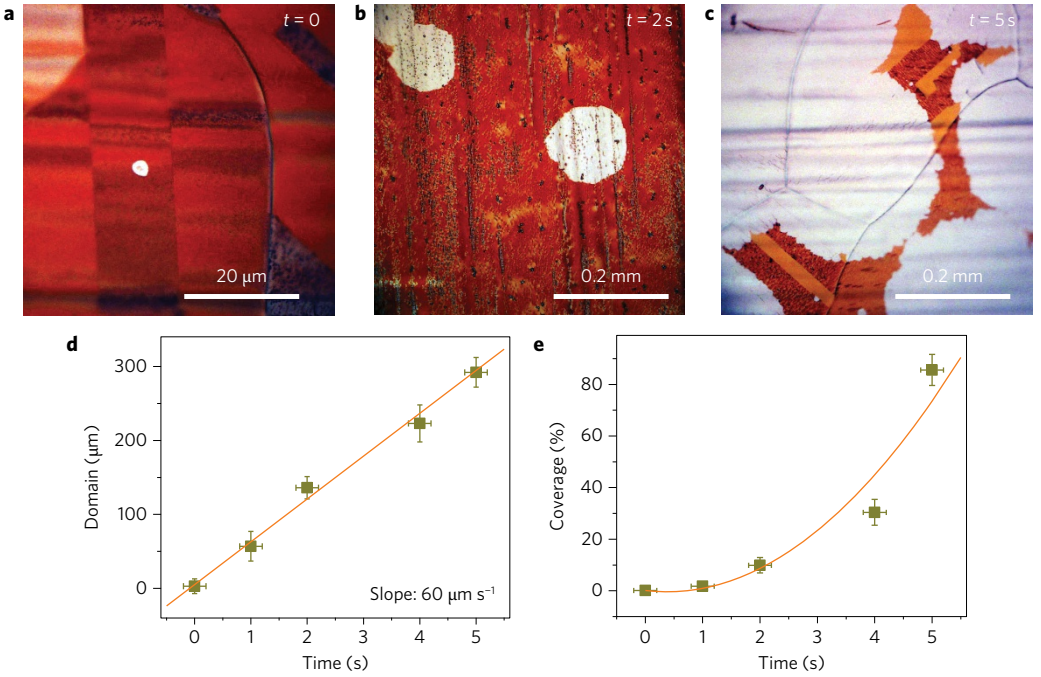

Figure 3 | Time evolution of graphene domain growth. a–c, Optical images of graphene synthesized at t = 0 s (**a**), 2 s (**b**) and 5 s (**c**), respectively. t = 0 s is defined as the moment when the graphene domain is large enough to be clearly visualized by optical microscopy. **d**, Plot and fit of the domain size of graphene as a function of growth time. The slope reveals an ultrafast growth rate of ~60 μm s^{-1}. **e**, Plot and fit of the coverage of graphene as a function of growth time. The coverage shows a quadratic dependence on the growth time, which reveals that no new nucleation centres form during the growth process. The error bars represent the standard error from measurements of 20 samples.

the shape of the graphene from fractal to star-shaped and then to rounded hexagonal domains[30]. As expected, the growth time required to form a sizable domain becomes very short or the growth becomes extremely fast when the carbon flux is sufficiently large.

The above analysis clearly shows that both the rounded graphene domain shape and the ultrafast graphene growth could be attributed to the greatly enhanced carbon flux. So we expect that the continuous supply of oxygen from the oxide substrate to the Cu surface would greatly enhance the decomposition of the feedstock (CH_4 molecules). To prove this assumption, we calculated the dissociation process of CH_4 on a Cu(100) surface, which is the critical step in feedstock decomposition, with (Fig. 4j) and without (Fig. 4l) the appearance of oxygen atoms on the Cu 100) surface (see Supplementary Method 2 for the simulation details). The result is shown in Fig. 4k. From the calculation, we can see that the barrier to CH_4 dissociation on a bare Cu(100) surface through the reaction of

$$CH_4 \xrightarrow{Cu} CH_3 + H \quad (3)$$

is 1.57 eV, whereas the barrier to CH_4 dissociation through the reaction of

$$CH_4 + O \xrightarrow{Cu} CH_3 + HO \quad (4)$$

on the oxygen attached Cu(100) surface is only 0.62 eV. Obviously, the significant reaction barrier reduction (of 0.95eV) could greatly promote the rate of CH_4 dissociation on the Cu surface and thus will drastically increase the concentration of CH_3 radicles and as well as those of CH_2, CH and C by the further dissociation of CH_3, CH_2 and CH, respectively.

As a brief estimation, let us reasonably assume that the coverage of oxygen atoms on the Cu(100) surface is in the range of c = 0.01 to 0.1, then the rate of CH_4 decomposition on the oxygen-rich Cu(100) could increase by

$$c\exp(0.95\,\mathrm{eV}/k_B T) \sim 57-570 \quad (5)$$

where k_B is the Boltzmann constant and T is the growth temperature. So we can estimate that, with the appearance of oxygen on the Cu surface, the carbon precursor flux can be increased by a few orders of magnitude. The greatly increased carbon flux will enhance the growth rate through the quick supply of the carbon precursor near the grown edge of the graphene. By considering this point together with other well-established roles of oxygen in graphene CVD growth on a Cu surface (lowering nucleation density[8–10] and reducing the energy barrier to carbon precursor attachment to the edge of graphene[9]), the enhanced growth rate can be explained. Here we note that except for the trapped oxygen released from the oxide substrates, the trapping of sublimated Cu vapour in the narrow gap will lead to a smooth Cu surface and thus a lower nucleation density and the enhanced diffusion of the carbon precursor on the Cu surface[31], which may help to enhance the growth rate as well. However, our control experiments show that its contribution to ultrafast growth is not significant under our growth conditions (Supplementary Fig. 5).

The ultrafast growth of graphene (close to the theoretical limit) opens an avenue for the scalable production of high-quality graphene films. For example, the fast, continuous and massive production of graphene film could be achieved by combining the process with the roll-to-roll[32] and stacking methods; and inch-sized single-crystal graphene samples could be synthesized within several minutes by combining with the point carbon source injector method[17] or around 10 s by using monocrystalline Cu(111) foils as the catalyst substrate[15].

In conclusion, we have demonstrated a CVD method assisted by a continuous oxygen supply to achieve ultrafast growth of large graphene single crystals. We synthesized 0.3-mm-sized graphene domains in just 5 s with a growth rate of 60 μm s^{-1}, more than two orders of magnitude faster than previous reported rates obtained

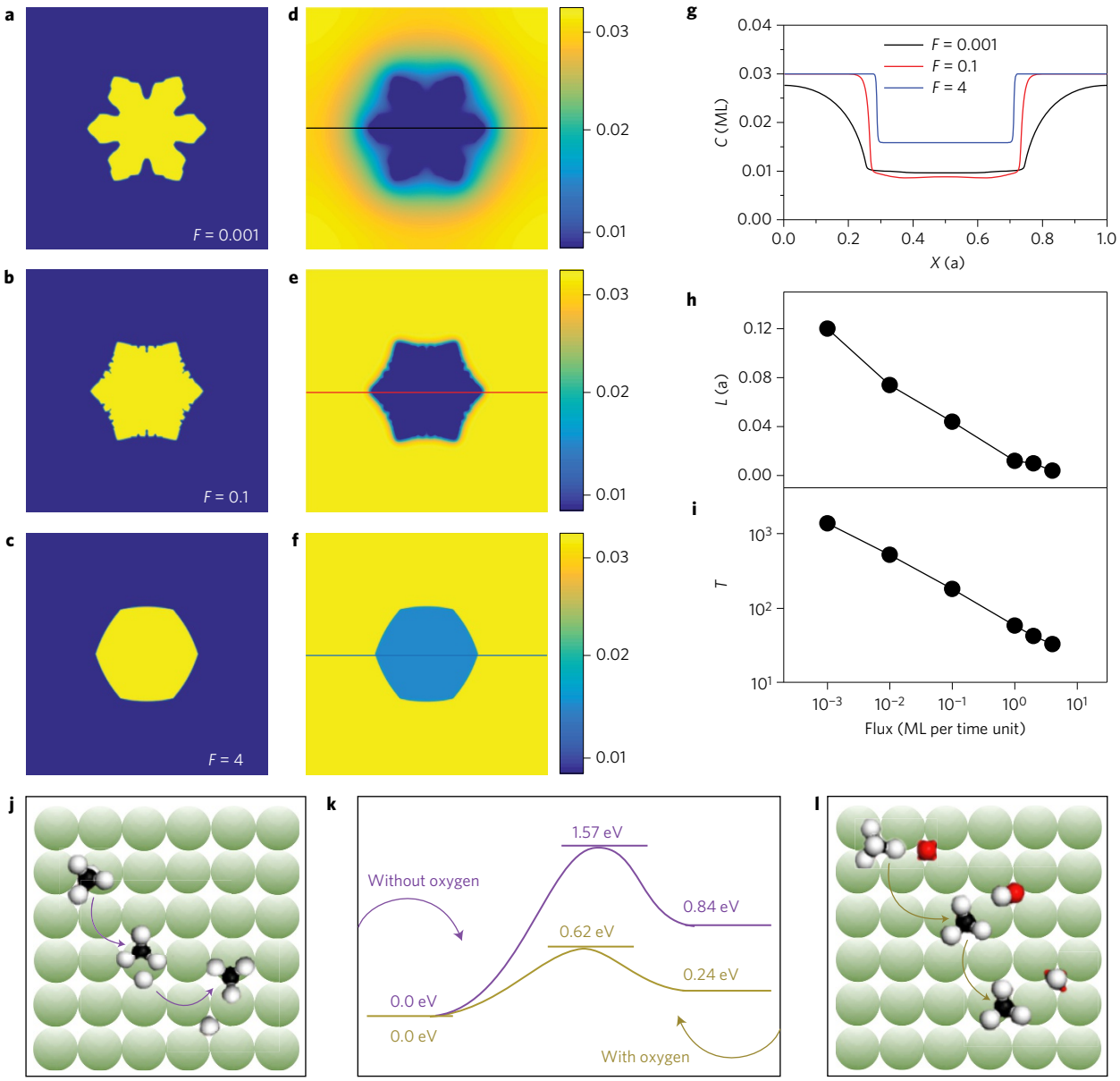

Figure 4 | The theoretical exploration of the mechanism of oxygen-assisted fast graphene growth on the Cu surface. a–f, Graphene domains (**a–c**) and concentration maps of the carbon precursor (**d–f**) on the substrate obtained by PFT simulations with carbon precursor landing rates of 0.001 (**a**,**d**), 0.1 (**b**,**e**) and 4 (**c**,**f**), respectively. **g**, The concentrations of the carbon precursor along the straight lines shown in **d–f**, where *C* is the concentration of carbon precursor in units of monolayer (ML) and *X* is the position along the lines in units of unit cell size, a. **h**,**i**, The width of the depletion zone (in units of unit cell length, a) (**h**) and the time required to grow a graphene domain with 1/4 coverage on the substrate (**i**) versus the *C* flux, the unit of *T* is defined as the period that is required for the accumulated flux to be one monolayer under the flux of 1. **j**,**l**, The decomposition reactions of $CH_4 \rightarrow CH_3 + H$ (**j**) and $CH_4 + O \rightarrow CH_3 + OH$ (**l**) on the Cu(100) surface with and without oxygen atoms, respectively. The white, red, black and green spheres represent H, O, C and Cu atoms, respectively. **k**, The energy barriers to CH_4 decomposition with and without oxygen are 0.62 and 1.57 eV, respectively.

from methods where graphene is grown on Cu foils. This ultrafast growth is driven by the continuous supply of oxygen that is released from the oxide substrate and by the confined gap between the Cu and the oxide. Our results provide a new direction for the synthesis of large single-crystal graphene wafers in very short timescales, which is very important for large-scale graphene industrial applications.

Methods

Methods and any associated references are available in the online version of the paper.

Received 30 October 2015; accepted 15 June 2016; published online 8 August 2016

References

1. Novoselov, K. S. *et al.* Two-dimensional gas of massless Dirac fermions in graphene. *Nature* **438**, 197–200 (2005).
2. Castro Neto, A. H. *et al.* The electronic properties of graphene. *Rev. Mod. Phys.* **81**, 109–162 (2009).
3. Zhang, Y. B. *et al.* Direct observation of a widely tunable bandgap in bilayer graphene. *Nature* **459**, 820–823 (2009).
4. Kim, K. *et al.* A role for graphene in silicon-based semiconductor devices. *Nature* **479**, 338–344 (2011).
5. Novoselov, K. S. *et al.* A roadmap for graphene. *Nature* **490**, 192–200 (2012).
6. Wang, H. *et al.* Controllable synthesis of submillimeter single-crystal monolayer graphene domains on copper foils by suppressing nucleation. *J. Am. Chem. Soc.* **134**, 3627–3630 (2012).

7. Yan, Z. *et al.* Toward the synthesis of wafer-scale single-crystal graphene on copper foils. *ACS Nano* **6**, 9110–9117 (2012).
8. Gan, L. & Luo, Z. T. Turning off hydrogen to realize seeded growth of subcentimeter single-crystal graphene grains on copper. *ACS Nano* **7**, 9480–9488 (2013).
9. Hao, Y. F. *et al.* The role of surface oxygen in the growth of large single-crystal graphene on copper. *Science* **342**, 720–723 (2013).
10. Zhou, H. L. *et al.* Chemical vapour deposition growth of large single crystals of monolayer and bilayer graphene. *Nature Commun.* **4**, 2096 (2013).
11. Mohsin, A. *et al.* Synthesis of millimeter-size hexagon-shaped graphene single crystals on resolidified copper. *ACS Nano* **7**, 8924–8931 (2013).
12. Wu, T. R. *et al.* Triggering the continuous growth of graphene toward millimeter-sized grains. *Adv. Funct. Mater.* **23**, 198–203 (2013).
13. Wang, C. C. *et al.* Growth of millimeter-size single crystal graphene on Cu foils by circumfluence chemical vapor deposition. *Sci. Rep.* **4**, 4537 (2014).
14. Miseikis, V. *et al.* Rapid CVD growth of millimetre-sized single crystal graphene using a cold-wall reactor. *2D Mater.* **2**, 014006 (2015).
15. Nguyen, V. L. *et al.* Seamless stitching of graphene domains on polished copper (111) foil. *Adv. Mater.* **27**, 1376–1382 (2015).
16. Babenko, V. *et al.* Rapid epitaxy-free graphene synthesis on silicidated polycrystalline platinum. *Nature Commun.* **6**, 7536 (2015).
17. Wu, T. R. *et al.* Fast growth of inch-sized single-crystalline graphene from a controlled single nucleus on Cu-Ni alloys. *Nature Mater.* **15**, 43–47 (2016).
18. Zhang, R. F. *et al.* Growth of half-meter long carbon nanotubes based on schulz-flory distribution. *ACS Nano* **7**, 6156–6161 (2013).
19. Yuan, Q. H., Hu, H. & Ding, F. Threshold barrier of carbon nanotube growth. *Phys. Rev. Lett.* **107**, 156101 (2011).
20. Gao, J. *et al.* Graphene nucleation on transition metal surface: structure transformation and role of the metal step edge. *J. Am. Chem. Soc.* **133**, 5009–5015 (2011).
21. Hata, K. *et al.* Water-assisted highly efficient synthesis of impurity-free single-walled carbon nanotubes. *Science* **229**, 1362–1364 (2004).
22. Gottardi, S. *et al.* Comparing graphene growth on Cu(111) versus oxidized Cu (111). *Nano Lett* **15**, 917–922 (2015).
23. Ishizaka, A. & Shiraki, Y. Low-temperature surface cleaning of silicon and its application to silicon Mbe. *J. Electrochem. Soc.* **133**, 666–671 (1986).
24. Bignardi, L. *et al.* Microscopic characterisation of suspended graphene grown by chemical vapour deposition. *Nanoscale* **5**, 9057–9061 (2013).
25. Banszerus, L. *et al.* Ultrahigh-mobility graphene devices from chemical vapor deposition on reusable copper. *Sci. Adv.* **1**, e1500222 (2015).
26. Gao, L. B. *et al.* Face-to-face transfer of wafer-scale graphene films. *Nature* **505**, 190–194 (2014).
27. Duong, D. L. *et al.* Probing graphene grain boundaries with optical microscopy. *Nature* **490**, 235–239 (2012).
28. Zhao, P. *et al.* Self-limiting chemical vapor deposition growth of monolayer graphene from ethanol. *J. Phys. Chem. C* **117**, 10755–10763 (2013).
29. Kim, H., Saiz, E., Chhowalla, M. & Mattevi, C. Modeling of the self-limited growth in catalytic chemical vapor deposition of graphene. *New J. Phys.* **15**, 053012 (2013).
30. Gao, J. F. *et al.* Graphene nucleation on transition metal surface: structure transformation and role of the metal step edge. *J. Am. Chem. Soc.* **133**, 5009–5015 (2011).
31. Chen, S. S. *et al.* Millimeter-size single-crystal graphene by suppressing evaporative loss of Cu during low pressure chemical vapor deposition. *Adv. Mater.* **25**, 2062–2065 (2013).
32. Deng, B. *et al.* Roll-to-roll encapsulation of metal nanowires between graphene and plastic substrate for high-performance flexible transparent electrodes. *Nano Lett.* **15**, 4206–4213 (2015).

Acknowledgements

We are grateful to Z. Liu for the helpful comments. We thank F. Wang and T. Cao for their help revising the manuscript. This work was supported by the NSFC (51522201, 11474006, 21525310, 11234001, 11327902, 91433102, 91021007 and 11074005), the National Basic Research Program of China (2016YFA0300903, 2013CBA01603, 2014CB932500, 2012CB921300) and the National Program for Thousand Young Talents of China.

Author contributions

K.L. and X.X. conceived the project. K.L. supervised the project. X.X., Z.Z. and Z.H. conducted the growth experiment. X.X. performed STM, AES and LEED experiments. X.X., K.L., H.P., F.D., D.Y. and E.W. analysed the experimental data. Z.Z. and H.W. performed the transfer of the graphene. R.Q. and P.G. conducted the TEM experiments. Z.L., L.L., L.Z., H.S. and C.L. performed the electrical measurements. F.D., L.Q. and J.Z. performed theoretical calculations. All of the authors discussed the results and wrote the paper.

Additional information

Supplementary information is available in the online version of the paper. Reprints and permissions information is available online at www.nature.com/reprints. Correspondence and requests for materials should be addressed to F.D., H.P. and K.L.

Competing financial interests

The authors declare no competing financial interests.

Methods

Ultrafast growth of large single-crystal graphene domains. We grew large single-crystal graphene by the CVD method. Cu foils (25 or 127 μm thick, 99.8%, Alfa Aesar) without any pretreatment were placed on a flat oxide substrate and then together they were loaded into a CVD furnace (Hefei Kejing Company OTF1250). The system was heated to 1,000 °C in 1 h with Ar (500 sccm) followed by annealing in additional H_2 (5 sccm) for 40 min. Then CH_4 (5 sccm) was introduced as the carbon source for graphene growth for different durations. Finally the system was cooled down naturally with Ar (1,000 sccm). The strong Ar flow helps to remove the residual CH_4 and accelerate the cooling rate. The system was kept at atmospheric pressure. We typically used a CH_4/H_2 ratio of 1:1 and CH_4 flow of 5 sccm in our growth process and found that tuning the ratio or the flow rate can provide different graphene domain morphologies (Supplementary Fig. 6).

Graphene transfer. Wet etching of the Cu foil was performed to transfer the graphene samples onto the SiO_2/Si substrates and TEM grids. In a typical transfer process, 8% PMMA (polymathic methacrylate, 350 K) in an anisole solution was spin coated onto the surface of the Cu foils and baked at 120 °C for 2 mins. After that the Cu was etched by a saturated $FeCl_3$ solution, resulting in a free-standing PMMA/graphene film floating on the surface of the solution. The film was thoroughly washed with HCl and deionized water and then transferred to the target substrates. The PMMA film was removed by acetone vapour, and then the substrate with graphene was rinsed with isopropyl alcohol and finally blow dried with N_2 gas.

Graphene electrical device fabrication. Six-terminal graphene Hall bars were fabricated using standard electron-beam lithography (EBL) followed by O_2 plasma etching. To this end, graphene samples were first transferred onto a 300 nm Si/SiO_2 substrate with prefabricated marks and further patterned into the device geometry by EBL and O_2 plasma etching. The Pd/Au contact electrodes were patterned via EBL, electron-beam evaporation of the metal and lift-off processes.

Graphene characterization

Optical measurements. Raman spectra were taken by a LabRAM HR800 system with a laser excitation wavelength of 633 nm and power of 1 mW. Optical images of the graphene on Cu (annealed in air at 200 °C for 5 min) were taken by an Olympus microscope (Olympus BX51).

AES, LEED and TEM measurements. AES was performed using a Riber MAC 2 system in a UHV under a base pressure below 3×10^{-7} Pa. LEED was performed using an Omicron LEED system in a UHV under a base pressure below 3×10^{-7} Pa. All of the LEED patterns were obtained with an electron energy of 60 eV. The SAED patterns were obtained by a FEI TECNAI T20 operated at 200 keV.

Electrical measurements. The electrical measurements were carried out in an Oxford cryostat instrument with a variable temperature (1.4–300 K) insert. The magnetic field (up to 14 T) was perpendicularly applied to the sample surface. Electrical signals were measured via low-frequency lock-in techniques. A Keithley 2,400 was used to apply the backgate voltage on the Si substrate and to measure the leakage currents.